

# Extending HELENA to incompressible plasma rotation parallel to the magnetic field

G. Poulipoulis<sup>1</sup>, G. N. Throumoulopoulos<sup>1</sup>, C. Konz<sup>2</sup>, and ITM-TF Contributors\*

<sup>1</sup>Physics Department, University of Ioannina, 451 10 Greece

<sup>2</sup>Max-Planck Institut für Plasma Physics, 85748 Garching bei München, Germany

## Abstract

Plasma rotation in connection to both zonal and mean (equilibrium) flows can play a role in the transitions to the advanced confinement regimes in tokamaks, as the L-H transition and the formation of Internal Transport Barriers. For incompressible rotation the equilibrium is governed by a generalized Grad-Shafranov (GGS) equation and a decoupled Bernoulli-type equation for the pressure. For parallel flow the GGS equation can be transformed to one identical in form with the usual GS equation. In the present study on the basis of the latter equation we have extended HELENA, an equilibrium fixed boundary solver. The extended code solves the GGS equation for a variety of the two free-surface-function terms involved for arbitrary Alfvén Mach and density functions. We have constructed diverted-boundary equilibria pertinent to ITER and examined their characteristics, in particular as concerns the impact of rotation on certain equilibrium quantities. It turns out that the rotation and its shear affect noticeably the pressure and toroidal current density with the impact on the current density being stronger in the parallel direction than in the toroidal one. Also, the linear stability of the equilibria constructed is examined by applying a sufficient condition.

## 1 Introduction

Plasma rotation affects the equilibrium, stability and transport properties of the plasma of a tokamak device. This has been established experimentally as well as theoretically. The appearance of highly peaked density, pressure and temperature profiles, the suppression of some instabilities and the creation of transport barriers, either in the edge region (H-mode) or inside the plasma core (Internal Transport Barriers), are associated with plasma flow (see for example [2], [3] and the review papers [4]-[5]). The transport barriers appear to be necessary ingredient towards the fully non-inductive operation of a future reactor [6]. The flows can be driven externally in connection with electromagnetic

---

\*See [1]

power and neutral beam injection for plasma heating and current drive or can be created spontaneously (intrinsic flows). Though it is not fully understood how the flow affects the confinement properties and especially the formation of transport barriers, the mode decorrelation and the reduction of turbulence play a significant role. Lately there is evidence that the rotation shear is more important than the flow itself, a fact that re-establishes flow as a key factor for the future big machines as ITER and later DEMO in which due to the large plasma volume it would be difficult to induce large flow velocities. However, the intrinsic rotation in these machines can be important [7]. A possible driving mechanism for the creation of intrinsic rotation in JET is the pressure gradient [8].

The MHD equilibria of axisymmetric plasmas, which can be starting points of stability and transport studies, is governed by the well known Grad-Shafranov (GS) equation. In addition to analytic solutions of this equation, as the Solovév solution, a number of fixed and free boundary codes have been developed to solve this equation in realistic situations for arbitrary choices of the free functions involved including information from experimental data. In connection with the present study we refer to the HELENA code, a finite element fixed boundary solver of the GS equation in the Integrated Tokamak Modelling-Task Force (ITM-TF) infrastructure. The code is described in Sec. 3. In the presence of flow the equilibrium satisfies a generalized Grad-Shafranov (GGS) equation together with a Bernoulli equation involving the pressure [9, 10]. For compressible flows the GGS equation can be either elliptic or hyperbolic depending on the value of a Mach number associated with the poloidal velocity. Note that the toroidal velocity is inherently incompressible because of axisymmetry. In that case the GGS equation is coupled with the Bernoulli equation through the density which is not uniform on magnetic surfaces. A number of codes have been developed to solve the set of these two equations mainly in the first elliptic region which is experimentally accessible <sup>1</sup>, as DIVA [11, 12], FINESSE [13] and FLOW [14]. In these codes either an adiabatic or an isothermal equation of state is adopted associated respectively with either isentropic or isothermal magnetic surfaces. For incompressible flow the density becomes a surface quantity and the GGS equation (Eq. (1) below) becomes elliptic and decouples from the Bernoulli equation (see Sec. 2). Consequently one has to solve an easier and well posed elliptic boundary value problem. In particular for fixed boundaries, convergence to the solution is guaranteed under mild requirements of monotonicity for the free functions involved in the GGS equation [15]. Therefore, it is reasonable to extend existing static equilibrium codes for incompressible flows of arbitrary direction. Also, it may be noted that uniformity of the density on magnetic surfaces is compatible with the TRANSP code [16] which assumes the density as a flux function. However, it should be clarified that since density deviations on magnetic surfaces have been observed experimentally, both compressible and incompressible equilibrium codes help in obtaining a more complete physical understanding.

The stability of fluids and plasmas in the presence of equilibrium flows non parallel to the magnetic field remains a tough problem reflecting to the lack of necessary and sufficient conditions. Only for parallel flows few sufficient

---

<sup>1</sup>For a typical thermonuclear plasma and magnetic field of the order of 1 Tesla, the plasma velocity is of the order of  $10 - 10^2$  Km/sec which lies well within the first elliptic region.

conditions for linear stability are available (e.g. [17]-[18]). Also, stability in the framework of normal mode analysis leads to a complex eigenvalue problem due to the antisymmetric properties of the force operator associated with the convective flow term in the momentum equation. Despite this difficulty, normal-mode-based stability studies have revealed that plasma flow can be a stabilising factor for the resistive wall mode [19, 20, 21, 22] by mitigating the mode while in turn the mode is braking the rotation. The rotation threshold, under which the mode is observed, appears to be a small fraction of the Alfvén frequency, though the experimental results on that point are not clear [20]. In addition, a connection between the plasma rotation and the error field is believed to affect the stabilization of the mode. Regarding the neoclassical tearing modes, reducing plasma rotation results in a deterioration of stability and an increase in the size of saturated islands [23, 24]. Therefore plasma rotation seems to be a key element for most -if not all- of the Advanced Tokamak Scenarios.

The aim of the present study is to extend the well known and widely used code HELENA [25] for incompressible rotation parallel to the magnetic field and to evaluate the impact of rotation on the equilibrium characteristics. It is noted that poloidal equilibrium flow components are included in the ITM-TF for the first time. The extension of the code is based on Eq. (1) which under an integral transformation can be put in a form identical with the usual GS equation. In addition we will examine the linear stability of the equilibria constructed by means of a pertinent sufficient condition [26].

The report is organised as follows. The GGS equation for plasmas with incompressible flow is reviewed in Sec. 2. In Sec. 3 the HELENA code is extended for rotation parallel to the magnetic field, particular equilibria are constructed and the impact of rotation and its shear on certain equilibrium quantities is examined. The linear stability of the equilibria constructed is studied by applying the stability condition of Ref. [26] in Sec. 4 and the results are compared with those of previous studies mainly based on analytic equilibrium solutions. Section 5 summarises the main conclusions.

## 2 Generalized Grad Shafranov equation

The equilibrium of a magnetically confined plasma with incompressible flow of arbitrary direction satisfies the following generalized GS equation (GGS) [27, 28]:

$$\begin{aligned} (1 - M_p^2)\Delta^*\psi - \frac{1}{2}(M_p^2)'|\nabla\psi|^2 + \frac{1}{2}\left(\frac{X^2}{1 - M_p^2}\right)' \\ + \mu_0 R^2 P_s' + \mu_0 \frac{R^4}{2} \left[\frac{\rho(\Phi')^2}{1 - M_p^2}\right]' = 0 \end{aligned} \quad (1)$$

Here, the poloidal magnetic flux function  $\psi(R, z)$  labels the magnetic surfaces, where  $(R, \phi, z)$  are cylindrical coordinates with  $z$  corresponding to the axis of symmetry;  $M_p(\psi)$  is the Mach function of the poloidal fluid velocity with respect to the poloidal Alfvén velocity;  $X(\psi)$  relates to the toroidal magnetic field,  $B_\phi = I/R$ , through  $I = X/(1 - M_p^2)$ ;  $\Phi(\psi)$  is the electrostatic potential; for vanishing flow the surface function  $P_s(\psi)$  coincides with the pressure;  $B$  is the magnetic field modulus which can be expressed in terms of surface functions

and  $R$ ;  $\Delta^* = R^2 \nabla \cdot (\nabla / R^2)$ ; and the prime denotes derivatives with respect to  $\psi$ . Because of incompressibility the density  $\rho(\psi)$  is also a surface quantity and the Bernoulli equation for the pressure decouples from (1):

$$P = P_s(\psi) - \varrho \left( \frac{v^2}{2} - \frac{R^2 (\Phi')^2}{1 - M_p^2} \right) \quad (2)$$

where  $v$  is the velocity modulus. The quantities  $M_p(\psi)$ ,  $X(\psi)$ ,  $P_s(\psi)$ ,  $\rho(\psi)$  and  $\Phi(\psi)$  are free functions. Derivation of Eq. (1) is based on the following two steps: first express the divergence free fields ( $\mathbf{B}$ ,  $\mathbf{j}$  and  $\rho \mathbf{v}$ ) in terms of scalar quantities and second, project the momentum equation,  $\rho(\mathbf{v} \cdot \nabla) \mathbf{v} = \mathbf{j} \times \mathbf{B} - \nabla P$ , and Ohm's law, along the toroidal direction,  $\mathbf{B}$  and  $\nabla \psi$ . The projections yield four first integrals in the form of surface quantities and Eqs. (1) and 2. Details are given in [27]-[29]. As already mentioned in Sec. 1 the decoupling of the GS equation from the pressure equation due to the incompressibility is the major difference between the current work and other models considering compressible flows associated with alternative equations of state. In the latter cases, the pressure equation needs to be solved simultaneously with the GS equation, while in our case, one has to just solve the GS under appropriate boundary conditions. Then, the Bernoulli equation is used as a formula to obtain the pressure.

Eq. (1) can be simplified by the transformation

$$u(\psi) = \int_0^\psi [1 - M_p^2(f)]^{1/2} df \quad (3)$$

under which (1) becomes

$$\Delta^* u + \frac{1}{2} \frac{d}{du} \left( \frac{X^2}{1 - M_p^2} \right) + \mu_0 R^2 \frac{dP_s}{du} \quad (4)$$

$$+ \mu_0 \frac{R^4}{2} \frac{d}{du} \left[ \rho \left( \frac{d\Phi}{du} \right)^2 \right] = 0 \quad (5)$$

Note that no quadratic term as  $|\nabla u|^2$  appears any more in (5). It is emphasized that once a solution of (5) is obtained, the equilibrium can be completely constructed with calculations in the  $u$ -space by employing (3), and the inverse transformation

$$\psi(u) = \int_0^u [1 - M_p^2(f)]^{-1/2} df \quad (6)$$

Specifically one finds

$$P = P_s(u) - \varrho(u) \left[ \frac{v^2}{2} - R^2 \left( \frac{d\Phi(u)}{du} \right)^2 \right] \quad (7)$$

$$\vec{B} = I(\psi) \vec{\nabla} \phi - \vec{\nabla} \phi \times \vec{\nabla} \psi = I(u) \vec{\nabla} \phi - \frac{d\psi}{du} \vec{\nabla} \phi \times \vec{\nabla} u \quad (8)$$

$$\vec{J} = \frac{1}{\mu_0} \left( -\Delta^* \psi \vec{\nabla} \phi + \vec{\nabla} \phi \times \vec{\nabla} I(\psi) \right) = \frac{d\psi}{du} R^2 \vec{\nabla} \left( \frac{\vec{\nabla} u}{R^2} \right) + \vec{\nabla} u \cdot \vec{\nabla} \frac{d\psi}{du} + \frac{dI(u)}{du} \vec{\nabla} \phi \times \vec{\nabla} u \quad (9)$$

$$\vec{E} = -\vec{\nabla} \Phi = -\frac{d\Phi(\psi)}{d\psi} \vec{\nabla} \psi = -\frac{d\Phi(u)}{du} \vec{\nabla} u \quad (10)$$

For parallel flows ( $\Phi' = 0$ ), Eq. (5) reduces in form to the usual GS equation. Also, in this case it can be shown that the poloidal, toroidal and total velocity Alfvén Mach numbers are exactly equal; henceforth the total velocity Mach number will be indicated by  $M$ . Moreover, in this case, setting

$$\varrho \vec{v} = K \vec{B} \quad (11)$$

where  $K$  is a scalar function, applying the divergence operator and taking into account the continuity equation,  $\vec{\nabla} \cdot (\varrho \vec{v}) = 0$ , one obtains  $\vec{\nabla} K \cdot \vec{B} = 0$  which means that the free function  $K$  is a surface quantity [30]

$$K = K(\psi)$$

Making use of Eq. (11) the Bernoulli equation 2, in the case of parallel plasma rotation can be written as

$$P = P_s(\psi) - \frac{1}{2\mu_0} M^2 B^2(\psi, R) = P_s(u) - \frac{1}{2\mu_0} M^2 B^2(u, R) \quad (12)$$

### 3 Extension of the HELENA code

The code HELENA, is a fixed boundary equilibrium solver [31] available on the EFDA ITM Gateway and used for ITM-TF purposes. The static GS equation used in the code is written as:

$$\Delta^* \psi = -F \frac{dF}{d\psi} - \mu_0 R^2 \frac{dP}{d\psi} = -\mu_0 R j_{tor} \quad (13)$$

HELENA solves Eq. (6) for a toroidal axisymmetric plasma by use of isoparametric bicubic Hermite finite elements. The main ingredients of the numerical algorithm is the Galerkin method, a non linear iteration scheme leading to a set of linear equations for each step of the iteration, and the use of straight field line coordinates. The function  $\psi$  is specified to assume a certain value on a predefined boundary which for HELENA is the last closed flux surface of its computational domain. This numerical technique yields very accurate solutions and has good convergence properties. Details are provided in [32].

Comparison of (5) for parallel plasma rotation ( $\Phi' = 0$ ) with (13) implies the following correspondence:

$$\psi \longleftrightarrow u \quad (14)$$

$$F \frac{dF}{d\psi} \longleftrightarrow \frac{1}{2} \frac{d}{du} \left( \frac{X^2}{1 - M^2} \right) \quad (15)$$

$$P(\psi) \longleftrightarrow P_s(u) \quad (16)$$

Therefore, the solver of the static code HELENA can be used to calculate the stationary equilibrium for parallel plasma rotation, though the output will no longer correspond to the “natural” quantities in the  $\psi$ -space. In order to preserve compatibility with the conventions established in the former EFDA ITM-TF the calculated by the solver quantities (now in the  $u$ -space) must be mapped to the “natural”  $\psi$ -space. For the mapping one must consider the following correspondence for the basic quantities:

Table 1: Values of some of the basic quantities of shot 35441.

$R_0$	$B_{\phi 0}$	$I_{plasma}$	$q_{min}$	$\beta_t$	$\psi_{axis}$	$\psi_{bound}$
6.34 m	5.178 T	14.46 MA	0.86	0.0103	0.0 Wb	79.09 Wb

$$P_{\text{HELENA}} \longleftrightarrow P_s \quad (17)$$

$$F_{\text{HELENA}} \longleftrightarrow \frac{X}{\sqrt{1-M^2}} \quad (18)$$

$$\psi_{\text{HELENA}} \longleftrightarrow u \quad (19)$$

By using Eqs. (8), (9) for  $\Phi' = 0$ , Eq. (12) and (17)-(19), we get the following expressions for the magnetic field, current density and pressure.

$$\vec{B} = \frac{F_{\text{HELENA}}}{\sqrt{1-M^2}} \vec{\nabla} \phi - \frac{1}{\sqrt{1-M^2}} \vec{\nabla} \phi \times \vec{\nabla} u \quad (20)$$

$$\vec{J} = \left[ \frac{-1}{\sqrt{1-M^2}} \Delta^* u + \frac{1}{2} \frac{1}{(1-M^2)^{3/2}} \frac{dM^2}{du} |\vec{\nabla} u|^2 \right] \vec{\nabla} \phi + \frac{d}{du} \left( \frac{F_{\text{HELENA}}}{\sqrt{1-M^2}} \right) \vec{\nabla} \phi \times \vec{\nabla} u \quad (21)$$

$$P = P_{\text{HELENA}} - \frac{1}{2\mu_0 R^2} \frac{M^2}{1-M^2} \left( F_{\text{HELENA}}^2 + |\vec{\nabla} u|^2 \right) \quad (22)$$

where the subscript HELENA refers to the computed by the solver quantities.

It is emphasized that any solution of (13), and therefore of the extended code, holds for arbitrary Mach numbers  $M(u)$  and densities  $\rho(u)$ . We have obtained a variety of equilibria by running the extended code. An example showing the magnetic surfaces of an ITER-relevant solution associated with input values of Table 1 is given in Fig. 1. This input for the solver is the 35441 shot of the ITM database within the infrastructure of the former EFDA ITM-TF. The input parameters of the code remained the same and together with the boundary, the pair of the free flux functions  $P'$  and  $FF'$  were chosen as input along the geometric centre, the vacuum magnetic field and  $\psi$  at the boundary. The results were obtained by means of a simple Kepler workflow which reads the input CPO of the shot, runs the HELENA code and stores the results in a CPO saved in the user's local database. It must be noted here that all the quantities that are stored in the CPO are in the  $\psi$ -space either via the transformation (such as the current densities, the pressure etc. as mentioned before) or by directly applying the inverse transformation (6), such as the poloidal flux function  $\psi$ .

To construct completely particular equilibria we have made several choices of the free function  $M^2(u)$ , e.g.,

$$M^2 = M_0^2 (u^m - u_b^m)^n \quad (23)$$

$$M^2 = C \left[ \left( \frac{u}{u_b} \right)^m \left( 1 - \left( \frac{u}{u_b} \right) \right) \right]^n \quad (24)$$

with

$$C = M_0^2 \left( \frac{m+n}{m} \right)^m \left( \frac{n}{m+n} \right)^n$$

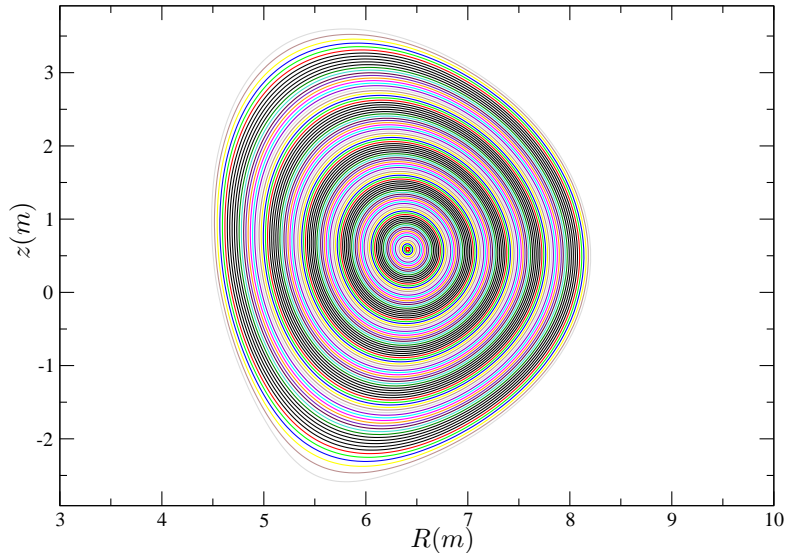


Figure 1: The magnetic surfaces of a paramagnetic equilibrium associated with the values of Table 1. The magnetic axis is located at  $(R_a = 6.4099 \text{ m}, z_a = 0.588 \text{ m})$  where the toroidal magnetic field is 5.77 T with respective vacuum value 5.178 T. The integral transformation (3) leaves the magnetic surfaces intact; therefore this configuration is unaffected by rotation as long as the input to the code is kept fixed.

Here,  $u_b$  refers to the plasma boundary; the free parameter  $M_0^2$  correspond to the maximum value of  $M^2$ ; and  $m$  and  $n$  are related to flow shear and the position of the maximum  $M^2$ . In particular, (23) is peaked on- while (24) peaked off-axis in connection with respective auxiliary heating of tokamaks. Note that for parallel rotation there is no need to specify the density because it can be eliminated. Plots of  $M$  in connection to (23) and (24) for different values of the free parameters are given in Figs. 2 and 3 respectively. In general the rotation has a rather weak contribution to Eq. (5). However, as already mentioned in Sec. 1, it is the velocity shear that is more important for the transition to improved confinement regimes in tokamaks than the velocity amplitude.

It is noted here that although Eq. (5) (with  $\Phi' = 0$ ) is identical in form with (13) we benchmarked the extended code against a generalized Solovév solution for parallel rotation involving  $M^2$  [33]. The agreement is very good as shown in Figs. 4 and 5 for the pressure and the toroidal current density respectively.

By varying the rotation parameters ( $M_0$ ,  $n$ ,  $m$ ) of the Mach number profile we examined the effect of rotation in certain of the basic equilibrium quantities. It is noted here that we consider the system without external momentum and energy sources and therefore the total energy of the system is kept constant regardless of the the nature of the rotation. Also, in the case of intrinsic rotation

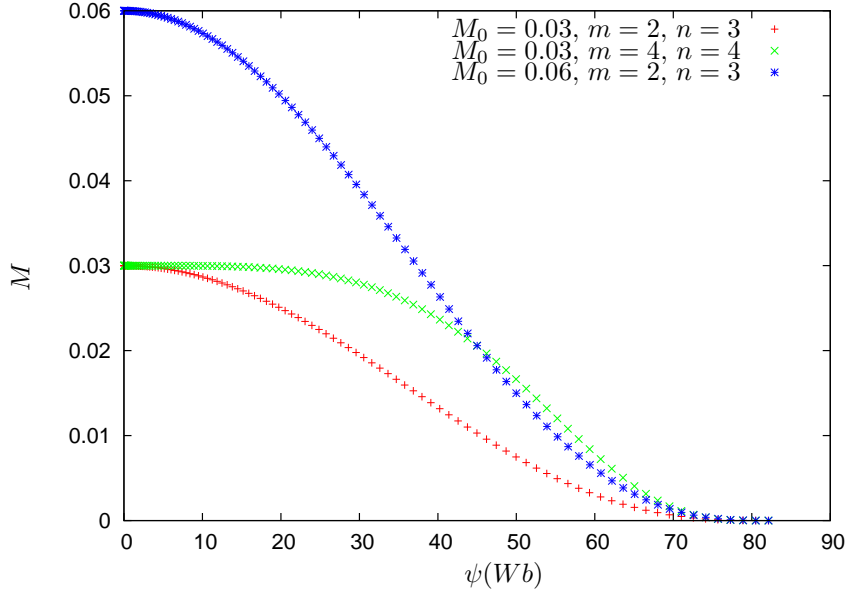


Figure 2: Plots of the on-axis peaked Mach number profile (Eq. (23)) with respect to  $\psi$  for various values of the profile parameters.

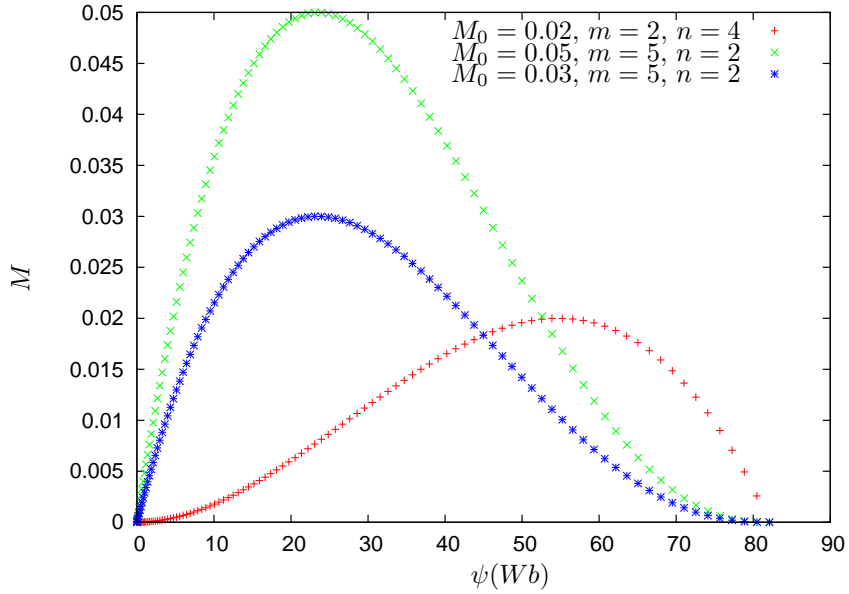


Figure 3: Plots of ITER-relevant off-axis peaked Mach number profiles (Eq. (24)) with respect to  $\psi$  for various values of the free parameters.

sources are not necessary. This is consistent with a desirable long term operation of a tokamak reactor after potential initial external energy and momentum



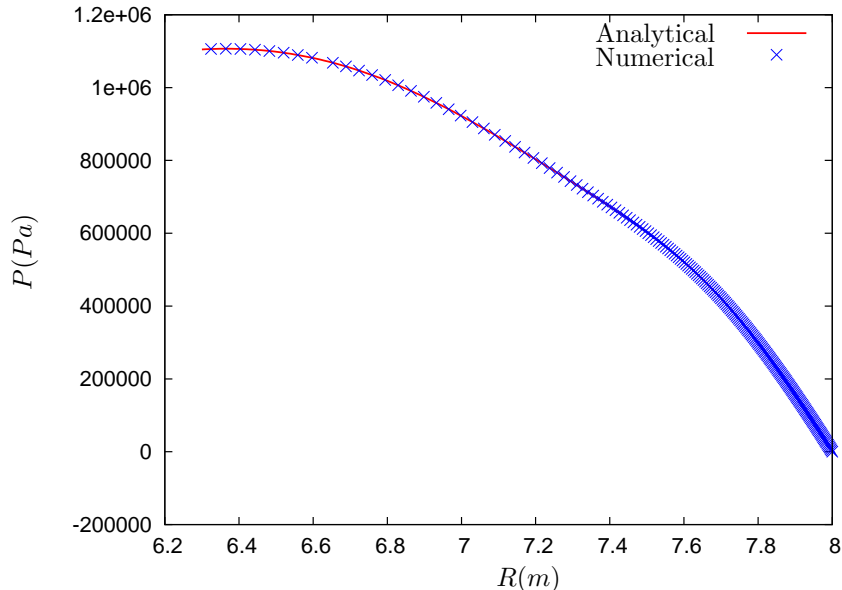


Figure 4: Plots of the pressure with respect to the radial distance from the axis of symmetry at the midplane  $z = 0$  for the generalized Solovév solution of Ref. [33] and the numerical one for the peaked on-axis Mach number profile (23) with  $M_0 = 0.1$ ,  $n = 2$ ,  $m = 3$ .

sources have been removed.

Regarding the pressure, on the basis of Eq. (22) for given  $P_s$  plasma rotation is expected to reduce the pressure values in comparison with the static ones. It appears that both the values of the Mach number and the shear of its profile affect the pressure. This result is different than that from code DIVA [12] due either to the direction of the rotation or to compressibility. It is worth noting that in the case of the off-axis localised rotation (Fig. 6), the effect on the pressure profile is significant compared to the on-axis case (Fig. 7) for the same values of  $M_0$ ,  $n$  and  $m$ . This is reasonable since in the off-axis case the values of the Mach number profile in Eq. (22) away from the magnetic axis are comparably larger than the on-axis-profile ones with respect to the static pressure term. Though for experimentally accessible velocity values on axis the effect on the pressure profile is small, the change in the shape of the profile can possibly affect the growth rate of pressure gradient driven modes as well as the intrinsic rotation [8]. This also holds for the off-axis rotation; also the values of the  $M_0$  that affect significantly the pressure are possibly accessible experimentally. In addition this type of profile is more probable for ITER which will exhibit a larger moment of inertia compared to present day tokamaks [34]. One more notable point is that for off-axis rotation the pressure profile is compatible with experimental results associated with the formation of either Internal Transport Barriers or edge barriers (H-mode). Specifically the pressure profile exhibits a steepness region where the maximum of the Mach number profile is located. In fact plasma rotation is associated with mode decorrelation

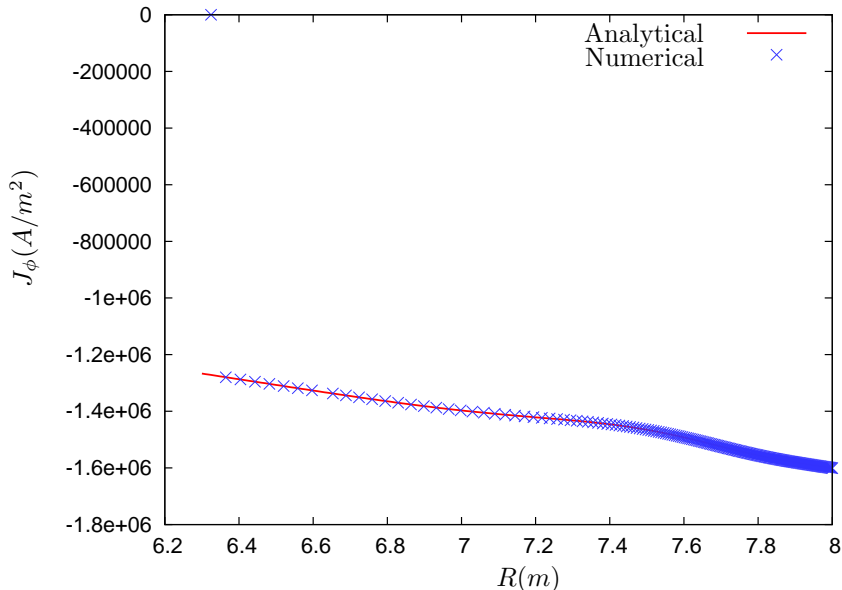


Figure 5: Plots of the toroidal current density with respect to the radial distance from the axis of symmetry at the midplane  $z = 0$  for the generalized Solovév solution of Ref. [33] and the numerical one for the peaked on-axis Mach number profile (23) with  $M_0 = 0.1$ ,  $n = 2$ ,  $m = 3$ .

Table 2: Values of the  $\beta_{tor}$  for various rotation cases.

Static	On-axis		Off-axis	
	$M_0 = 0.03$ $m = 3$ $n = 3$	$M_0 = 0.03$ $m = 4$ $n = 4$	$M_0 = 0.05$ $m = 5$ $n = 2$	$M_0 = 0.02$ $m = 2$ $n = 4$
0.0100	0.0091	0.0089	0.0075	0.0093

resulting in the reduction of transport coefficients and eventually the formation of a transport barrier. On physical grounds, the increase of the steepness of the pressure profile is related with the formation of this barrier in connection with the flow. Also, since the rotation decreases the pressure and increases the toroidal magnetic field (see Eqs. (7) and (20)) it is expected that in the presence of rotation the toroidal beta will decrease. Both the maximum value of  $M^2$  and its shear contribute to this reduction as indicated by the results quoted in Table 2.

Paying attention to the current density, one can conclude that the off-axis rotation affects the profiles more than the on-axis as can be seen in Figs. 8- 11. This implies that the rotation shear is more important for the shaping of the plasma current density than the rotation itself. Therefore even for small values of the Mach number the impact of rotation shear on the current density can be significant. Comparison of Figs. 8-10 and 9-11 shows that for each individual Mach number profile the impact of parallel rotation on the parallel current density is stronger than on the toroidal component of the current density. This indicates that there is a correlation of the direction of the rotation and the

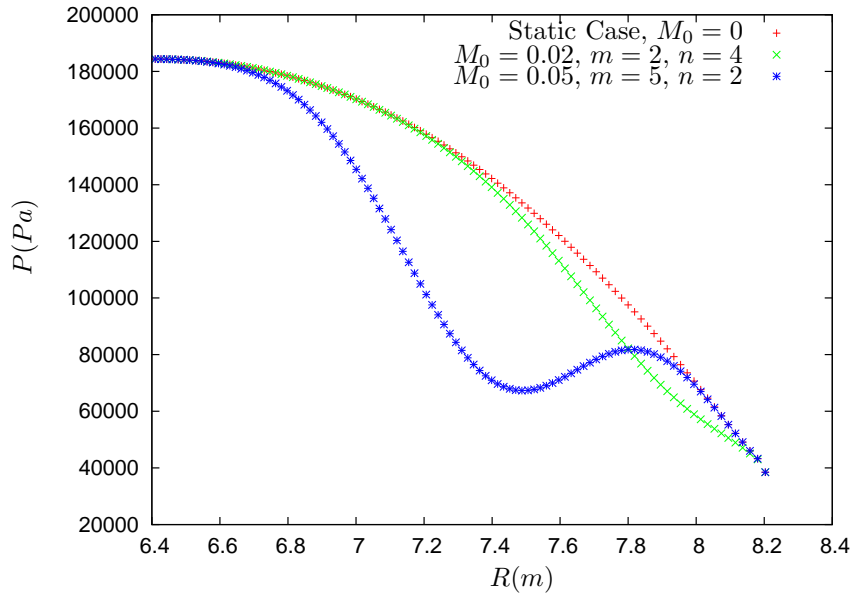


Figure 6: Plots of the pressure with respect to the radial distance from the axis of symmetry at the midplane  $z = 0$  for various Mach number profiles peaked off-axis.

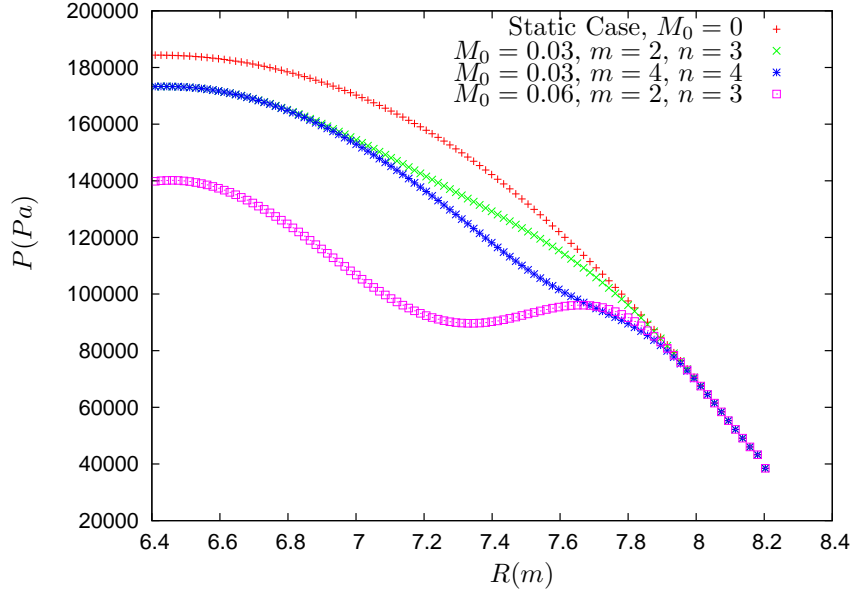


Figure 7: Plots of the pressure with respect to the radial distance from the axis of symmetry on the midplane  $z = 0$  for various Mach number profiles peaked on-axis.

corresponding direction of the current density. Experimentally, the co-current direction of rotation results in better quality ITBs for the electron temperature [35]. Analysing the current density in two components, a toroidal and a poloidal one, we can conclude that the plasma rotation affects more the poloidal component of the current density than the toroidal one. Taking into account that the plasma rotation is parallel to the magnetic field and the toroidal component of  $\vec{B}$  is dominant over the poloidal one we conclude that also the toroidal component of the rotation is the dominant over the poloidal one and in turn affects the poloidal current density more than the toroidal current density.

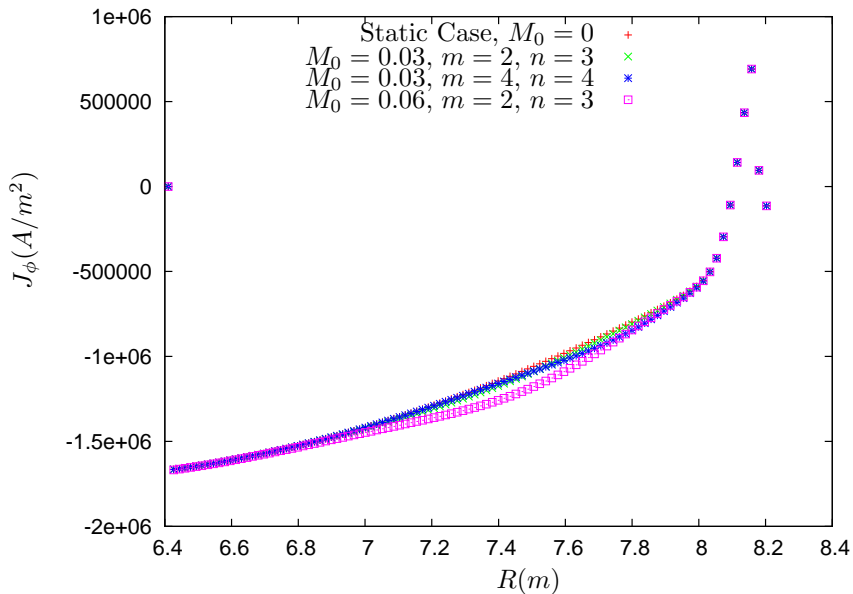


Figure 8: Plots of the toroidal current density versus the radial distance from the axis of symmetry on the midplane  $z = 0$  for various Mach number profiles peaked on-axis.

## 4 Stability consideration

We now consider the important issue of linear stability for the equilibria constructed with respect to small magnetohydrodynamic perturbations by applying the sufficient condition of [26, 36]. This condition states that a general steady state of a plasma of constant density and incompressible flow parallel to  $\vec{B}$  is linearly stable to small three-dimensional perturbations if the flow is sub-Alfvénic ( $M^2 < 1$ ) and  $A \geq 0$ , where  $A$  is given below by (25)-(29). Note here that if the density is uniform at equilibrium it remains so at the perturbed state because of incompressibility. For axisymmetric equilibria in the  $\psi$ -space  $A$  assumes the

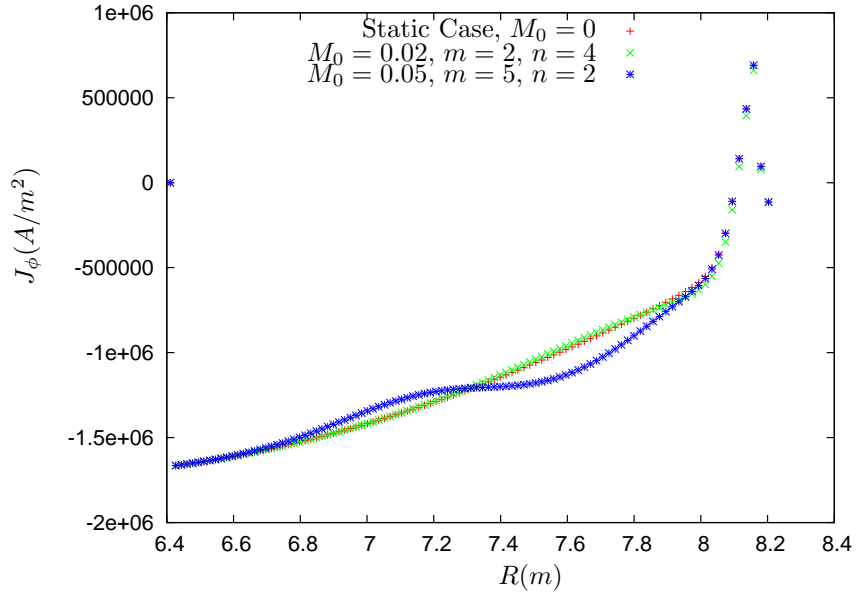


Figure 9: Plots of the toroidal current density versus the radial distance from the axis of symmetry on the midplane  $z = 0$  for various Mach number profiles peaked off-axis.

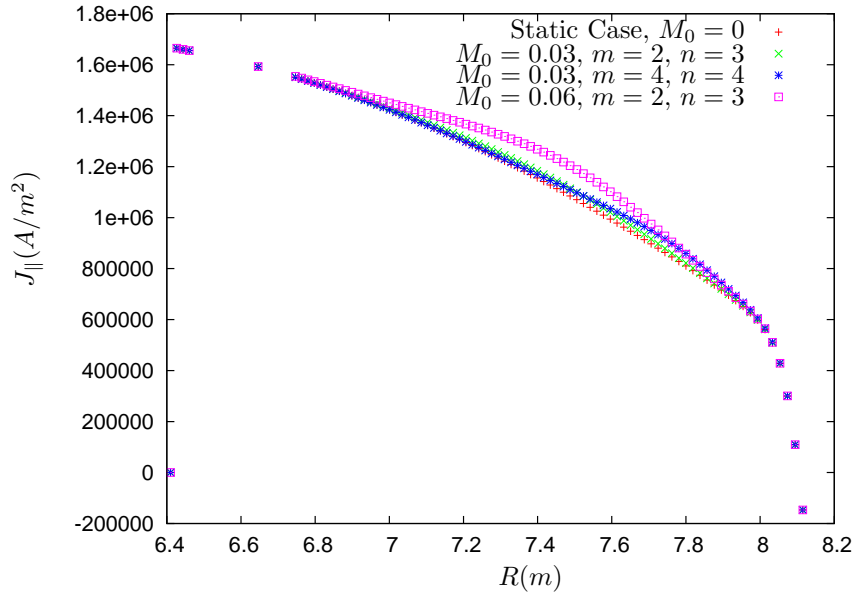


Figure 10: Plots of the parallel to the magnetic field current density versus the radial distance from the axis of symmetry on the midplane  $z = 0$  for various Mach number profiles peaked on-axis.

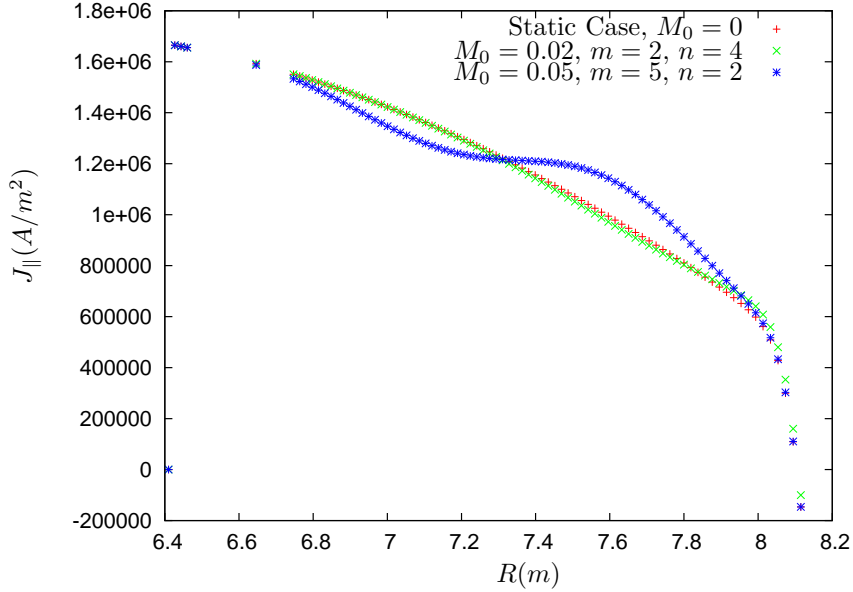


Figure 11: Plots of the parallel to the magnetic field current density versus the radial distance from the axis of symmetry on the midplane  $z = 0$  for various Mach number profiles peaked off-axis.

form

$$A = A_1 + A_2 + A_3 + A_4 \quad (25)$$

$$A_1 = -(1 - M^2)\mu_0^2(\vec{J} \times \vec{\nabla}\psi)^2 \quad (26)$$

$$A_2 = (1 - M^2)\mu_0(\vec{J} \times \vec{\nabla}\psi) \cdot (\vec{\nabla}\psi \cdot \vec{\nabla})\vec{B} \quad (27)$$

$$A_3 = -\frac{1}{2}\frac{dM^2}{d\psi}|\vec{\nabla}\psi|^2\left(\vec{\nabla}\psi \cdot \frac{\vec{\nabla}B^2}{2}\right) \quad (28)$$

$$A_4 = -\frac{1}{2}\frac{dM^2}{d\psi}|\vec{\nabla}\psi|^4g \quad (29)$$

$$g = \frac{1}{1 - M^2}\left(\frac{dP_s}{d\psi} - \frac{dM^2}{d\psi}\frac{B^2}{2\mu_0}\right)$$

with  $\vec{B}$  and  $\vec{J}$  given by Eqs. (20) and (21). The quantity  $A_1$  being always negative consists a destabilizing contribution potentially related to current driven modes. The other terms can be either stabilizing or destabilizing. Specifically, the term  $A_2$  relates to the current density and the variation of the magnetic field perpendicular to the magnetic surfaces.  $A_3$  and  $A_4$  are mostly flow terms because they vanish in the absence of flow.  $A_3$  additionally depends on the variation of the magnitude of the magnetic field perpendicular to the magnetic surfaces while  $A_4$  depends on the pressure gradient through the quantity  $g$ . The flows satisfying (5) are inherently sub-Alfvénic because of the transformation (3). Derivation of the condition is provided in [26]. Here it is just noted that

it comes from the global requirement of non-negativeness of an integrand unlike usual local requirements associated with stability criteria for static equilibria, e.g. the Mercier criterion for localized interchanged modes.

The condition was applied with the aid of Mathematica to equilibrium outputs from HELENA which were interpolated by 5<sup>th</sup> order splines assuring the necessary continuity of derivatives up to second order. Due to the fact that spline interpolation in Mathematica works only for structured grid an additional step was necessary. The appropriate output of HELENA was initially parsed to MATLAB which mapped it to a structured grid by means of Delaunay triangulation. The procedure was benchmarked against the Solovév solution showing accuracy up to order  $10^{-10}$ . The results show that for 17 flow profiles examined, including the static one, the condition is not satisfied within the plasma region. Evaluating the impact of plasma rotation on the midplane  $z = 0$  at the points where the Mach number exhibits its maximum and at the points where  $|dM/d\psi|$  is maximum we concluded that the rotation (through the terms  $A_3$  and  $A_4$ ) can be spatially in part destabilizing and in part stabilizing. Also,

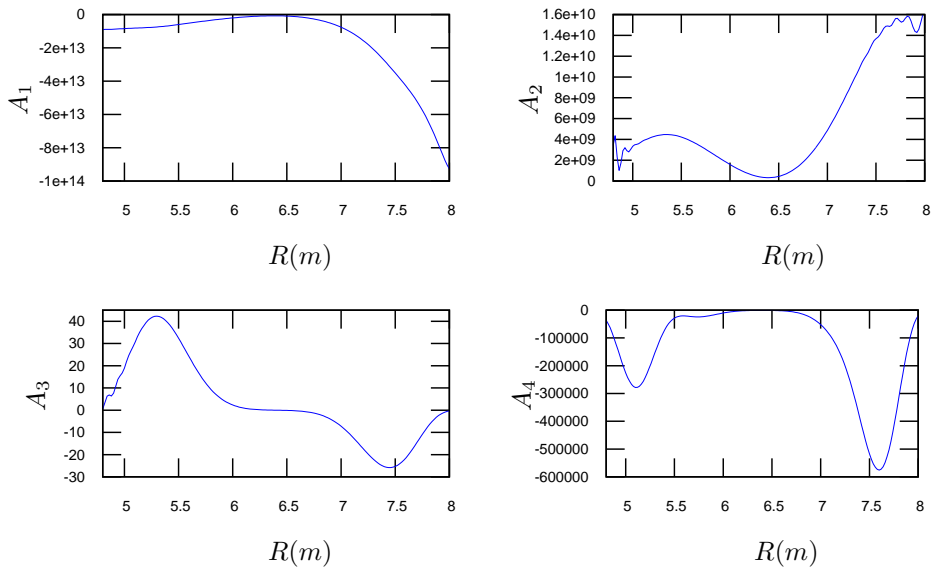


Figure 12: Plots of the quantities  $A_1 - A_4$  for a typical equilibrium with peaked on-axis Mach number (Eq. (23)) with  $M_0 = 0.06$ ,  $n = 2$ ,  $m = 3$ .

this can be seen in Fig. 12 where the individual terms consisting  $A$  are plotted on the mid-plane  $z = 0$ . The term  $A_2$  related the magnetic shear is stabilizing but can not overcome the destabilizing term  $A_1$ . Also, the flow term  $A_4$  has a weaker destabilizing contribution and  $A_3$  is stabilizing in the inner region close

to the axis of symmetry and destabilizing in the outer region. It should be clarified here that the term “stabilizing” (“destabilizing”) has the meaning of a non-negative (negative) contribution to  $A$ . However, since the condition is sufficient,  $A < 0$  does not imply instability but indecisiveness.

In previous studies we made a similar stability study on the basis of analytic or quasianalytic solutions of the GGS equation (5) for parallel rotation in plane [37], translational symmetric [38] and axisymmetric toroidal [39] geometries. In these studies it turned out that the condition  $A \geq 0$  is satisfied in a major part of the plasma. Stabilization is caused mainly by the term  $A_2$  in conjunction with equilibrium non-linearity with a weaker stabilizing contribution from the rotation and its shear. Also, certain results indicate that the equilibrium non-linearity activates flow stabilization. In the present case, the input profiles are linear and that may explain the destabilizing results. In other studies [40, 41] it turned out that the flow terms  $A_3$  or  $A_4$  are destabilizing. The above mentioned results and those of the present study clearly indicate that the impact of rotation and its shear on stability is far from universal; depending on the particular equilibria and the shape of the rotation profile the rotation can be either stabilizing or destabilizing.

## 5 Conclusions

We extended the HELENA fixed boundary equilibrium solver to equilibria with incompressible plasma rotation parallel to the magnetic field. The pertinent GGS equation by means of an integral transformation is put in a form identical to the usual static GS equation. This transformation which maps the poloidal magnetic flux function  $\psi$  to another flux function  $u$  leaves the shape of the magnetic flux surfaces intact just relabelling them. Via this and the inverse transformation the calculated by the solver quantities in the  $u$  space, are mapped to the  $\psi$ -space. The code was run in the EFDA ITM-TF infrastructure with input shot 35441 developed for ITER simulations. A simple workflow in the Kepler environment was used for reading the input CPO of the shot and storing the results locally in the user’s database.

On the basis of the equilibria constructed by the extended code we examined the impact of rotation and its shear on the pressure, toroidal current density and toroidal beta. As expected the pressure is reduced by the rotation. For localised flow the shape of the pressure profile resembles that observed in advanced confinement regimes. Specifically, owing to the plasma rotation, a rapid decrease in the pressure values accompanied by a flat region is evident around the maximum of the Mach number profile when this profile is peaked off-axis. The effect of peaked on-axis plasma rotation on the pressure profile is weaker due to the larger relative values of the pressure in the core region. The effect of rotation on the current density is similar to that on the pressure with the additional remark that the impact of the parallel to the magnetic field rotation is stronger on the poloidal current density than that on the toroidal one. This result suggests that there is correlation between the direction of the rotation components and the corresponding components of the equilibrium current density.

Furthermore, we examined the linear stability of the equilibria constructed by means of a sufficient condition. The results were inconclusive because the condition was satisfied nowhere in the plasma for a variety of the Mach num-



ber profiles examined. A detailed evaluation of the individual terms consisting the pertinent stability quantity  $A$  (Eqs. (25)-(29)) showed that the variation of the magnetic field perpendicular to the magnetic surfaces, related to the magnetic shear, is stabilizing but, for the equilibria considered, can not overcome a destabilizing contribution potentially related to current driven modes. Also, depending on the spatial position a weaker impact of the flow can be either stabilizing or destabilizing in consistence with previous stability studies.

It is interesting to extend further the code in two respects: First, for non parallel incompressible flow associated with electric fields which play a role in the transitions to improved confinement regimes. This can be done on the basis of Eq. (5) by including the  $R^4$ -term with the differential part of the equation remaining unaffected. Second, in the presence of pressure anisotropy which for compressible flows has already been considered in the FLOW code.

## 6 Acknowledgements

Part of this work was conducted during visits of two of the authors (G.P. and G.N.T.) to the Max-Planck-Institut für Plasmaphysik, Garching. The hospitality of that Institute is greatly appreciated.

This work has been carried out within the framework of the EUROfusion Consortium and has received funding from (a) the National Programme for the Controlled Thermonuclear Fusion, Hellenic Republic, (b) Euratom research and training programme 2014-2018 under grant agreement no. 633053. The views and opinions expressed herein do not necessarily reflect those of the European Commission.

## References

- [1] GL Falchetto, D Coster, R Coelho, BD Scott, L Figini, D Kalupin, E Nardon, S Nowak, LL Alves, JF Artaud, V Basiuk, João PS Bizarro, C Boulbe, A Dinklage, D Farina, B Faugeras, J Ferreira, A Figueiredo, Ph Huynh, F Imbeaux, I Ivanova-Stanik, T Jonsson, H-J Klingshirn, C Konz, A Kus, NB Marushchenko, G Pereverzev, M Owsiak, E Poli, Y Peysson, R Reimer, J Signoret, O Sauter, R Stankiewicz, P Strand, I Voitsekhovitch, E Westerhof, T Zok, W Zwingmann, ITM-TF Contributors, ASDEX Upgrade the Team, and JET-EFDA Contributors. The European Integrated Tokamak Modelling (ITM) effort: achievements and first physics results. *Nuclear Fusion*, (4):043018. doi: 10.1088/0029-5515/54/4/043018.
- [2] S Günter, RC Wolf, F Leuterer, O Gruber, M Kaufmann, K Lackner, M Maraschek, PJ Mc Carthy, H Meister, A Peeters, et al. Simultaneous attainment of high electron and ion temperatures in discharges with internal transport barriers in ASDEX upgrade. *Physical Review Letters*, (14): 3097.
- [3] F Romanelli, M Laxåback, et al. Overview of JET results. *Nuclear Fusion*, (9):094008.
- [4] K Itoh and SI Itoh. The role of the electric field in confinement. *Plasma Physics and Controlled Fusion*, (1):1-49.

- [5] CD Challis. The use of internal transport barriers in tokamak plasmas. *Plasma Physics and Controlled Fusion*, 46:B23–B40, December 2004. doi: 10.1088/0741-3335/46/12B/003.
- [6] ACC Sips, G Tardini, CB Forest, O Gruber, PJ Mc Carthy, A Gude, LD Horton, V Igochine, O Kardaun, CF Maggi, et al. The performance of improved H-modes at ASDEX Upgrade and projection to ITER. *Nuclear Fusion*, (11):1485.
- [7] WM Solomon, KH Burrell, R Budny, RJ Groebner, JE Kinsey, GJ Kramer, TC Luce, MA Makowski, D Mikkelsen, R Nazikian, et al. Momentum confinement at low torque. *Plasma Physics and Controlled Fusion*, (12B): B313.
- [8] L-G Eriksson, E Righi, and K-D Zastrow. Toroidal rotation in ICRF-heated H-modes on JET. *Plasma Physics and Controlled Fusion*, (1):27–42.
- [9] AI Morozov and LS Solov’ev. Steady-state plasma flow in a magnetic field. In *Reviews of Plasma Physics*, pages 1–103. Springer.
- [10] E Hameiri. The equilibrium and stability of rotating plasmas. *Physics of Fluids*, 26:230–237, January 1983. doi: 10.1063/1.864012.
- [11] S Semenzato, R Gruber, and HP Zehrfeld. Computation of symmetric ideal MHD flow equilibria. *Computer Physics Reports*, (7):389–425.
- [12] E Strumberger, S Günter, P Merkel, S Riondato, E Schwarz, C Tichmann, and HP Zehrfeld. Numerical MHD stability studies: toroidal rotation, viscosity, resistive walls and current holes. *Nuclear Fusion*, (9):1156.
- [13] AJC Beliën, MA Botchev, JP Goedbloed, B van der Holst, and R Keppens. FINESSE: Axisymmetric MHD Equilibria with Flow. *J. Comput. Phys.*, (1):91–117, October . ISSN 0021-9991. doi: 10.1006/jcph.2002.7153.
- [14] L Guazzotto, R Betti, J Manickam, and S Kaye. Numerical study of tokamak equilibria with arbitrary flow. *Physics of Plasmas*, (2):604–614, February . doi: 10.1063/1.1637918.
- [15] R Courant and D Hilbert. *Methods of mathematical physics vol. 2*. CUP Archive.
- [16] RV Budny, MG Bell, AC Janos, DL Jassby, LC Johnson, DK Mansfield, DC McCune, MH Redi, JF Schivell, G Taylor, TB Terpstra, MC Zarnstorff, and SJ Zweben. Simulations of alpha parameters in a TFTR DT supershot with high fusion power. *Nuclear Fusion*, 35:1497–1508, 1995. doi: 10.1088/0029-5515/35/12/I10.
- [17] S Friedlander and MM Vishik. On stability and instability criteria for magnetohydrodynamics. *Chaos: An Interdisciplinary Journal of Nonlinear Science*, (2):416–423.
- [18] PJ Morrison, E Tassi, and N Tronko. Stability of compressible reduced magnetohydrodynamic equilibria—Analogy with magnetorotational instability. *Physics of Plasmas*, (4):042109.

- [19] AM Garofalo, AD Turnbull, ME Austin, J Bialek, MS Chu, KJ Comer, ED Fredrickson, RJ Groebner, RJ La Haye, LL Lao, et al. Direct observation of the resistive wall mode in a tokamak and its interaction with plasma rotation. *Physical Review Letters*, (19):3811, .
- [20] AM Garofalo, GL Jackson, RJ La Haye, M Okabayashi, H Reimerdes, EJ Strait, JR Ferron, RJ Groebner, Y In, MJ Lanctot, et al. Stability and control of resistive wall modes in high beta, low rotation DIII-D plasmas. *Nuclear Fusion*, (9):1121, .
- [21] MS Chu and M Okabayashi. Stabilization of the external kink and the resistive wall mode. *Plasma Physics and Controlled Fusion*, (12):123001.
- [22] V Igochine. Physics of resistive wall modes. *Nuclear Fusion*, (7):074010. doi: 10.1088/0029-5515/52/7/074010.
- [23] PA Politzer, CC Petty, RJ Jayakumar, TC Luce, MR Wade, JC DeBoo, JR Ferron, P Gohil, CT Holcomb, AW Hyatt, et al. Influence of toroidal rotation on transport and stability in hybrid scenario plasmas in DIII-D. *Nuclear Fusion*, (7):075001.
- [24] RJ La Haye, DP Brennan, RJ Buttery, and SP Gerhardt. Islands in the stream: The effect of plasma flow on tearing stability. *Physics of Plasmas*, (5):056110.
- [25] C Konz, W Zwingmann, F Osmanlic, B Guillerminet, F Imbeaux, P Huynh, M Plociennik, M Owsiak, T Zok, and M Dunne. First physics applications of the Integrated Tokamak Modelling (ITM-TF) tools to the MHD stability analysis of experimental data and ITER scenarios. *EPS*, page O2, 2011. URL <http://ocs.ciemat.es/eps2011pap/pdf/02.103.pdf>.
- [26] GN Throumoulopoulos and H Tasso. A sufficient condition for the linear stability of magnetohydrodynamic equilibria with field aligned incompressible flows. *Physics of Plasmas*, (12):122104.
- [27] H Tasso and GN Throumoulopoulos. Axisymmetric ideal magnetohydrodynamic equilibria with incompressible flows. *Physics of Plasmas*, (6): 2378–2383.
- [28] G Poulipoulis, GN Throumoulopoulos, and H Tasso. Toroidal flow-caused change in magnetic topology of equilibrium eigenstates. *Physics of Plasmas*, (4):042112. doi: 10.1063/1.1867497.
- [29] GN Throumoulopoulos, H Tasso, and G Poulipoulis. Side-conditioned axisymmetric equilibria with incompressible flows. *Journal of Plasma Physics*, 74:327–344, June 2008. doi: 10.1017/S0022377807006769.
- [30] GN Throumoulopoulos and H Tasso. On axisymmetric resistive magnetohydrodynamic equilibria with flow free of Pfirsch-Schlüter diffusion. *Physics of Plasmas*, 10:2382–2388, June 2003. doi: 10.1063/1.1571542.
- [31] GTA Huysmans, JP Goedbloed, and W Kerner. Isoparametric bicubic Hermite elements for solution of the Grad-Shafranov equation. *International Journal of Modern Physics C*, (01):371–376.

- [32] C Konz and R Zille. *Manual of HELENA Fixed Boundary Equilibrium Solver*. Max-Planck Institute for Plasma Physics, 2007.
- [33] Ch Simintzis, GN Throumoulopoulos, G Pantis, and H Tasso. Analytic magnetohydrodynamic equilibria of a magnetically confined plasma with sheared flows. *Physics of Plasmas*, (6):2641–2648.
- [34] Peter C de Vries, M-D Hua, DC McDonald, C Giroud, M Janvier, MF Johnson, T Tala, K-D Zastrow, and JET EFDA Contributors. Scaling of rotation and momentum confinement in JET plasmas. *Nuclear Fusion*, (6):065006.
- [35] N Oyama, A Isayama, T Suzuki, Y Koide, H Takenaga, S Ide, T Nakano, N Asakura, H Kubo, M Takechi, et al. Improved performance in long-pulse ELMy H-mode plasmas with internal transport barrier in JT-60U. *Nuclear Fusion*, (7):689.
- [36] VA Vladimirov and KI Ilin. The three-dimensional stability of steady magnetohydrodynamic flows of an ideal fluid. *Physics of Plasmas*, (12):4199–4204.
- [37] GN Throumoulopoulos, H Tasso, and G Poulipoulis. Magnetohydrodynamic ‘cat eyes’ and stabilizing effects of plasma flow. *Journal of Physics A Mathematical General*, 42:335501, August 2009. doi: 10.1088/1751-8113/42/33/335501.
- [38] Ap Kuiroukidis and GN Throumoulopoulos. Two-dimensional nonlinear cylindrical equilibria with reversed magnetic shear and sheared flow. *Journal of Plasma Physics*, 80:27–41, February 2014. doi: 10.1017/S0022377813000883.
- [39] Ap Kuiroukidis and GN Throumoulopoulos. Toroidal equilibrium states with reversed magnetic shear and parallel flow in connection with the formation of Internal Transport Barriers. *Journal of Plasma Physics*, (4):905810404, .
- [40] Ap Kuiroukidis and GN Throumoulopoulos. An analytic nonlinear toroidal equilibrium with flow. *Plasma Physics and Controlled Fusion*, (7):75003–75009, . doi: 10.1088/0741-3335/56/7/075003.
- [41] DA Kaltsas and GN Throumoulopoulos. Generalized Solovév equilibrium with sheared flow of arbitrary direction and stability consideration. *Physics of Plasmas*, page 084502.